Leonardo Electronic Journal of Practices and Technologies
ISSN 1583-1078
Issue 30, January-June 2017
p. 269-286

Engineering, Environment

Processing of pure titanium containing titanium-based reinforcing ceramics additives using spark plasma sintering

Saliou DIOUF, Mondiu Olayinka DUROWOJU, Mxolisi Brendon SHONGWE and Peter Apata OLUBAMBI

Institute for NanoEngineering Research, Department of Chemical and Metallurgical Engineering, Tshwane University of Technology Pretoria, South Africa
E-mail: modurowoju@lautech.edu.ng

Received: December 06, 2016 / Accepted: June 14, 2017 / Published: June 30, 2017

Abstract

The densification behaviour, microstructural changes and hardness characteristics during spark plasma sintering of CP-Ti reinforced with TiC, TiN, TiCN and TiB_2 were investigated. Commercially pure Ti powders were dry mixed with varied amounts (2.5 and 5 wt. %) of the ceramic additives using a T2F Turbula mixer for 5 h and at a speed of 49 rpm. The blended composite powders were then sintered using spark plasma sintering system (model HHPD-25 from FCT Germany) at a heating rate of 100ºC min^{-1}, dwell time of 5 min and sintering temperature of 950ºC. The sintering of CP-Ti was used as a base study to select the proper spark plasma sintering temperature for full density. Densification was monitored through analysis of the recorded punch displacement and the measured density of the sintered samples using Archimedes method. High densities ranging from 97.8% for 5% TiB_2 addition to 99.6% for 5% TiCN addition were achieved at a relatively low temperature of 950°C. Microstructural analyses show a uniform distribution of the additives and finer structure showing their inhibitive effect on grain growth. An improved hardness was observed in all the cases with highest values obtained with TiCN as a result of the combined effect of TiC and TiN. A change in the fracture mode from trans granular to intergranular was also observed.

Keywords

Spark plasma sintering; Titanium Matrix Composites; Ceramics; Densification; Microstructure

Introduction

Titanium matrix composites (TMCs) have recently attracted a lot of attention owing to their ability to retain their high strength and modulus at elevated temperatures as well as their good creep resistance and non-burning characteristics which made them materials of choice in many engineering applications. Discontinuously reinforced titanium may be obtained by embedding ceramic particles in a titanium matrix. This would result in an improvement on the mechanical and physical properties of the TMCs arising from their isotropic characteristics [1]. As such, the nature of the reinforcement, its particles' size and shape and amount influence the matrix/particle interfaces and therefore affect the physical and mechanical properties of the MMCs. Small reinforcement dimensions provide better mechanical properties and thermal stability, whereas large dimensions and high volumetric quantity improve wear resistance [2].

The choice of a suitable ceramic material for TMC production is very important as reinforcing ceramic can both affect the processing technique and service performance. For example SiC may partially dissolve in titanium and form non-stoichiometric unstable compounds, which is detrimental to the stability and mechanical properties of the TMCs. This applies as well to oxide as titanium cannot withstand oxygen levels above 0.4 wt. % [3]. This is not the case for other carbides, nitrides and elemental carbon whose dissolution by the titanium matrix forms stable carbide, boride and the metallic elements form a solid solution.

Ceramic particulates such as titanium carbide (TiC), titanium nitride (TiN), titanium carbonitride (TiCN) and titanium diboride (TiB_2) reinforced Ti matrix have been investigated in order to improve the mechanical properties. Among other technologies adopted is arc plasma [4], high energy electron-beam irradiation [5] and laser alloying [6] techniques. Makuch et al. [7] used Laser surface alloying to produce hard ceramic phases reinforced composite layers, titanium borides and titanium carbides, applying boron and carbon on commercially pure titanium. This led to the formation of TiB, TiB2 and TiC, which resulted in high micro hardness as depending on the percentage of these ceramic phases in more

plastic eutectic mixture, a high cohesion and significant increase in wear. Yazdi and Kashani-Bozorg [8] worked on the coating of h-BN-based powder mixture on commercially pure (CP)-Ti substrate using Tungsten inert gas (TIG) technique. The reaction of h-BN with titanium led to an in-situ hybrid composite layer formation showing near stoichiometric dendrites of TiN, platelets of TiB and interdendritic regions of α-Ti marten site crystal structures with improved micro hardness and a wear resistance four times greater than that of CP-Ti. Some researches considering a combination of these ceramics have also been reported. Yang et al. [9] in order to explore the in-situ synthesis of TiCN/TiN composite coating on the Ti-6Al-4V substrate used pulsed Nd:YAG laser and a precursor of Ti/C mixture powder with a certain mole ratio and a pure nitrogen gas. They also investigated the phase constituents, microstructure, micro hardness and wear resistance of the formed ceramic coating. The formation of $TiC_{0.3}N_{0.7}$, TiN, and $TiN_{0.3}$ with relative amounts depending on the laser power density, led to a significant improvement of both micro hardness and abrasion resistance.

Very recently a similar work using the reinforcement of Ti with TiC, TiN, TiCN particles processed by powder injection moulding (PIM) [10] was reported. After two hours of sintering in vacuum at 1300ºC, the addition of TiC, TiN and TiCN resulted in good adhesion between the matrix and reinforcement, providing some benefit in terms of densification with a highest value of 97.2% relative density, strength and hardness, but only a slight improvement in ductility was noticed. So far the use of TiC, TiN, TiCN and TiB_2 to reinforce Ti-based materials was focused on surface composites fabrication by depositing the ceramic powders on a Ti alloys substrate. However, their additions on Ti and processing by spark plasma sintering have been seldom reported.

The SPS system which combines a hot press and a pulse current generator has proven to be particularly suitable for sintering metals with highly stable oxides, as titanium and aluminium [11-14] even if no reducing atmosphere is used. The peculiarity of the heating mechanism in SPS which is induced by the application of a pulsed continuous current [15-16] is a prerequisite to densify materials of low self-diffusion rate such as TiB_2 which makes it difficult to sinter by conventional routes despite its excellent hardness, corrosion resistance and electrical conductivity. The temperature in SPS is measured in two regions: at low temperature (from room temperature to 1200ºC) using a thermocouple inserted inside the die wall and at high temperature (600-2000^{0}C) a pyrometer placed at the surface of the die is used. The measured temperature is therefore mostly different from that inside the sample.

This difference in temperature has been fully documented using finite element methods [17-18]. Despite the numbers of reported studies on SPS technique for producing a variety of ceramics reinforced metal matrix composites (MMC) and on Ti-based composites, it is observed that no studies have been reported on its application in sintering TMC.

The present work therefore aims at processing titanium reinforced with TiC, TiN, TiB_2 and TiCN using the SPS technique. The influences of the additives on densification, microstructure, phases, sintering and mechanical properties of the spark plasma sintered titanium are studied. Pure titanium, as a base material, was preliminarily sintered at different temperatures 900, 950 and 1000^0C to select the proper sintering temperature for full density. The singularity of the SPS model used in this research (model HHPD-25 from FCT Germany) resides in the position of the pyrometer at the upper punch at 5 mm of the surface of the sample which records temperatures close to that of the inside of the sample.

Materials and method

A commercially pure titanium (cP-Ti) powder (Alfa Aesar, -325 mesh, purity 99.5%), pure TiC (Alfa Aesar, 2-6 µm, purity 99.5%), TiN (Alfa Aesar, 1.15 µm, purity 99.5%), TiCN (HC Starck, < 4 µm, 50/50 C) and TiB_2 (HC Starck, < 4 µm, purity 99.5%) powders were used to produce Ti-based reinforcing ceramics additives. The four additives (TiC, TiN, TiCN and TiB_2) were dry mixed at room temperature with the cP-Ti using a Turbula Shaker Mixer T2F in varied mass ratios (2.5 and 5 wt. %) at a speed of 49 rpm for 5h. Scanning Electron Microscope (SEM) analysis was carried out to account for the dispersion of the additives, related microstructural changes and fractographic features using field emission gun scanning electron microscope (FEGSEM) (JEOL JSM-7600F).

The morphology of the as-received titanium powder can be observed in Fig. 1. The SEM micrograph show non-spherical particles in the range of – 44 µm with differences in shape.

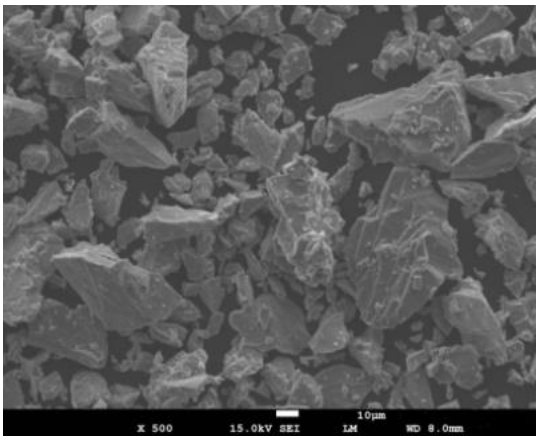

Figure 1. SEM micrograph the starting CP-Ti

X-ray diffraction (XRD) (model PANalytical EMPYREA) was carried out for phases and possible phases change using X'Pert HighScore Plus software. The XRD measurements were performed using CuKα radiation, a step size of 0.0821 and a counting time of 1 s in the 2θ range of 5 – 90 degrees.

The spark plasma sintering (SPS) system (model HHPD-25 from FCT Germany) with pulsed DC voltage (pulse cycle: 12 pulses ON/2 pulses OFF, duration 3 ms) was used to produce disks of 30 mm diameter and 5 mm height using graphite die and punches. A pressure P = 50 MPa was applied throughout the SPS cycle at a heating rate of 100^{o}C and a dwell time of 5 min at the sintering temperature. The cP-Ti was preliminarily sintered at different temperatures 900, 950 and 1000^{o}C to select the proper sintering temperature for full density which was found to be 950^{o}C.

The density of the sintered specimens was measured with the Archimedes method using the following equation (1):

$$\rho_m = \frac{\rho_a}{\rho_a - \rho_w}\rho_o \quad (1)$$

Where ρ_a is the mass of the composite in air, ρ_b is the mass of the same composite in distilled water and ρ_o is the density of the distilled water at room temperature (0.998 g/cm^3).

The relative density was calculated with reference to the theoretical density of the starting powders constituents using the rule of mixtures (Table 1). For microstructural analysis, the samples were cut and their cross-section was mounted, ground and polished and then etched using Kroll's reagent (3 mL HF, 6 mL HNO3 in 100 mL H_2O) prior to optical metallography (OM) examinations using a Nikon Eclipse LV150 optical microscope. Vickers micro hardness (Micro hardness tester FM – 800) was measured using a load of 0.5 N

(HV0.5, 500 gf) and a dwell time of 15 s. Ten (10) measurements were carried out on each specimen to have a better representation and around the middle of each specimen to avoid near-surface effects.

Results and discussion

Density and densification behaviour

The effect of TiC, TiCN and TiN at different mass ratios on density of the composites are shown in Table 1.

Table 1. Theoretical and relative densities of Ti reinforced with TiC, TiN, TiC and TiB_2

Initial composition	Theoretical density (g/cm^3)	Measured density (g/cm^3)	Relative density (%)
Ti	4.51	4.51	100.0
Ti-2.5 TiC	4.52	4.49	99.3
Ti – 5 TiC	4.53	4.50	99.3
Ti–2.5 TiN	4.53	4.50	99.3
Ti – 5 TiN	4.54	4.50	99.1
Ti–2.5 TiCN	4.52	4.50	99.6
Ti–5 TiCN	4.53	4.48	98.9
Ti–2.5 TiB_2	4.51	4.46	98.9
Ti – 5 TiB_2	4.51	4.41	97.8

It can be seen from Table 1 that full density for Ti can be reached with a sintering temperature of 950^0C at a heating rate of 100^0C/min and pressure of 50 MPa. Table 1 indicates a decrease of the relative density of Ti with the additions of the Ti-based ceramics. The relative density of the samples is above 99% of the samples except for the composite with 5 wt.% TiCN, 2. 5 wt.% TiB2 and 5 wt.% TiB2. Compositions with 2.5%TiC and 2.5%TiN attained a relative density of 99.3% while that of 2.5%TiCN additions is increased up to 99.6%. However, for 5% additions of the additives the obtained relative densities of TiC, TiN and TiCN reinforced titanium are 99.3, 99.1 and 98.9, respectively. The results showed that, except for TiC, an increase in the additions of Ti-based ceramics from 2.5 and 5 wt. % led to a decrease in the relative density of the resulting composite. This could be due to the fact that both the α-Ti and β-Ti phases dissolve carbon, nitrogen and boron but more of nitrogen and boron than carbon much more nitrogen than carbon [19]. The dissolution of nitrogen leads to

the formation of N_2 gas which results in pore formation and therefore to a density decrease. TiB_2 resulted in the formation of B_2O_3 (because of the strong affinity of boron for oxygen) which can only be totally removed at above 1500^0C (30).

The poorer densification which is found to further reduce when the amount of additives is increased can therefore be linked to the pore formation as a result of trapped B_2O_3 caused by its partial removal (Durowoju et al 2016). These results showed that an increase in the amount of additives result in a decrease of density except for TiC.

To assess the shrinkage behaviour during sintering, the shrinkage rate and temperature vs. time of the sintered bodies with and without additives was plotted as shown in Figure 2.

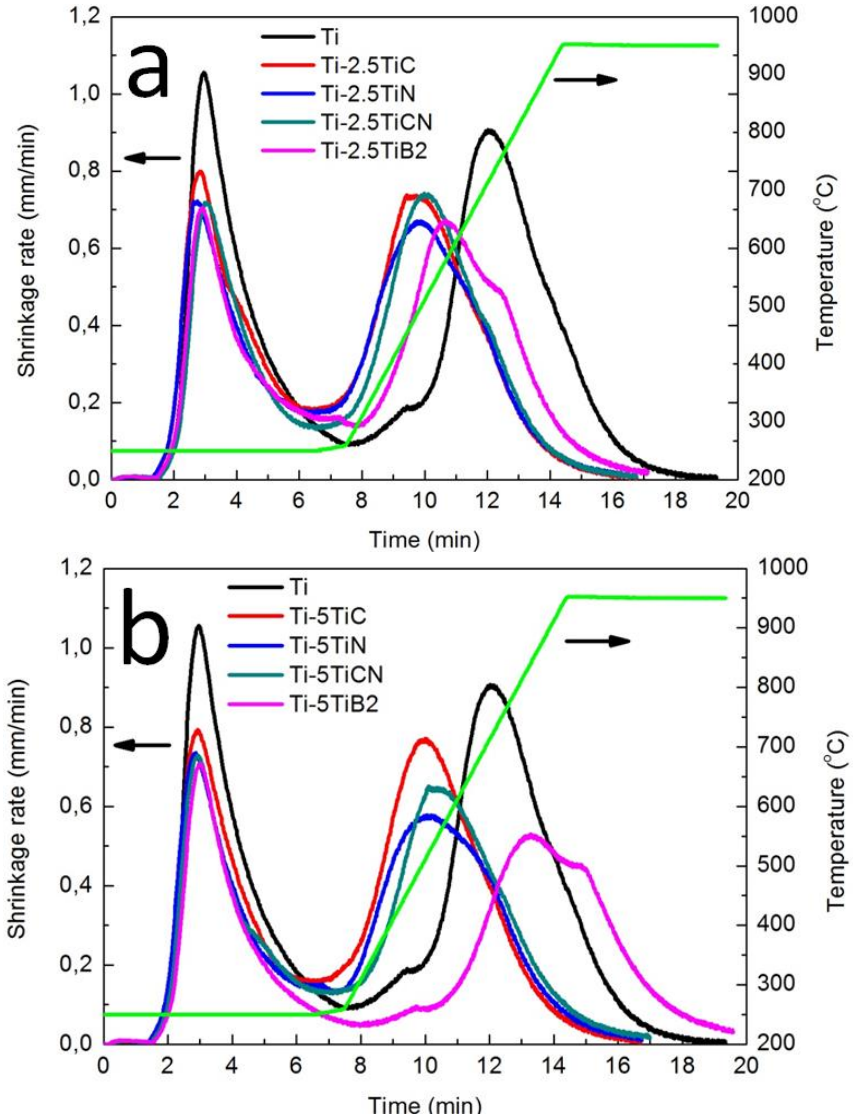

Figure 2. Shrinkage rate and temperature vs. time plots of the sintered compacts without and with: a) 2.5 wt. % and b) 5 wt. % Ti-based ceramic additives

The displacement rate of the piston, which is a record of the changes in the thickness of the specimen with respect to time, is an indication of the densification rate. During spark plasma sintering the phenomena responsible for densification are indicated in correspondence of three peaks of displacement rate: rearrangement of the particles, localized deformation at the contact points, and bulk deformation of the particles [20-21].

The shrinkage curves in Figure 2 show two main peaks at 250 and 773ºC and a third peak for pure Ti at 450ºC. This suggests that the three peaks observed in the case of pure Ti would correspond to powder particles rearrangement, localized deformation at the contact points and bulk deformation of the particles. However, in the case of the sintering of Ti with the addition of TiC, TiN and TiCN, there seems to be an overlapping between localized and bulk deformation phenomena as a result of the decrease of the maximum densification temperature.

The following can also be seen in Figure 2: a decrease of the shrinkage rate, the occurrence of the maximum densification at a shorter time and a reduction of the maximum densification temperature with the addition of the Ti-based ceramics. It can be also observed that the shrinkage rate decreases with an increase in the amount of the additives. These could be attributed to the high melting point of the additives.

The decrease on the particles rearrangement rate and an earlier occurrence of the localized/bulk deformation peak are possibly due to the hard nature of the additives and to the facilitation of surface diffusion during sintering as a result of the interactions between Ti and TiC, TiCN and TiN, respectively. TiB2 instead, has a similar behaviour to Ti with an extra peak at a temperature of 952ºC. At a 2.5 wt. %TiB2 addition (Figure 2a), both the localized and bulk deformation peaks occur earlier than in the case of pure Ti as a result of the increased surface diffusion with the addition of TiB2. An increase in the amount of TiB2 (from 2.5 to 5 wt. % TiB2) (Figure 2b), normalizes the localized deformation while slightly delaying the bulk deformation and decreases the shrinkage rate as a result of the hard nature of TiB2. TiB2 is found to experience parabolic oxidation kinetics below 1000ºC as a result of the formation of TiO2 and B2O3 [22] through the following equation: $TiB_2 + 5/2O_2 = TiO_2 + B_2O_3$ (Figures 5 and 6). B2O3 evaporates at 750ºC and the formed gas may be entrapped within the composite leading to porosity generation which therefore explains the relatively lower relation density of Ti/TiB2 and its decrease with an increased amount of TiB2. The

rutile form of TiO2, is a nonstoichiometric oxide with both titanium interstitial ions and oxygen vacancies which make it prone to oxidation through cationic and anionic movements. TiO2 also has a high Pilling Bedworth ratio of 1.95 which causes micro cracks and pores in the oxide scale due to compressive stresses in the oxide layer [23].

Microstructure analysis and XRD measurements

Microstructure of the SPS compacts

In order to analyse the microstructural and dispersion characteristics of the reinforcements, backscattered SEM images recorded from Ti with 2.5 and 5 wt. % of TiC, TiN, TiCN and TiB2 are shown in Fig. 3.

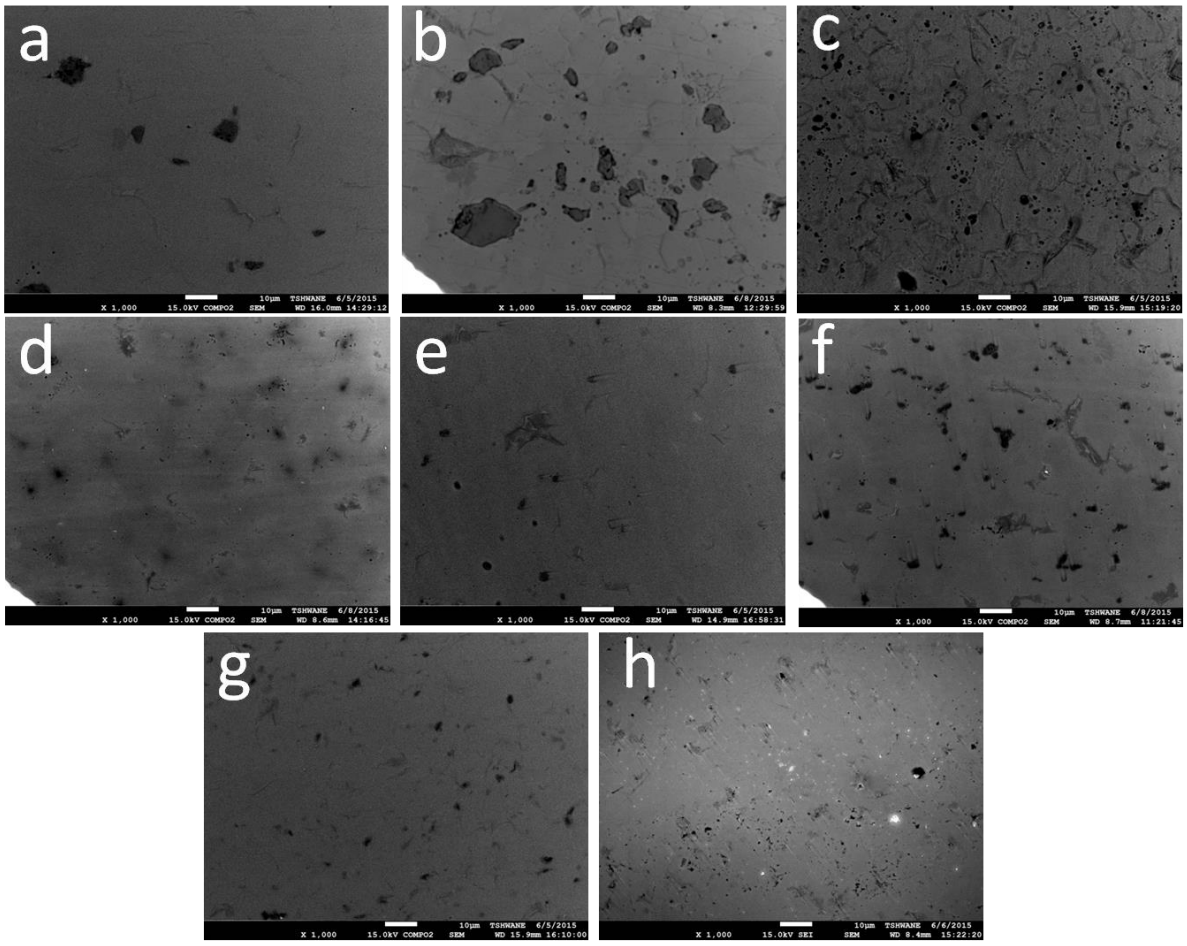

Figure 3. Backscattered SEM images of a) Ti-2.5TiC; b) Ti-5TiC; c) Ti-2.5TiN; d) Ti-5TiN; e) Ti-2.5TiCN, f) Ti-5TiCN, g) Ti-2.5TiB2 and h) Ti-5TiB2

Figure 3 show the microstructure of the spark plasma sintered Ti with Ti-based ceramic. In all the figures two distinct regions can be observed: one darker and one lighter. The darker regions which are the carbide-, nitride-, carbonitride - and boride-rich regions are uniformly distributed throughout the Ti matrix (lighter region). A certain level of porosity

which varies with the type of additives is observable. As SPS is a solid-state sintering process, diffusion of C, N and B in the matrix is expected to occur for a desirable microstructure with improved properties to be formed. The high interaction during sintering between Ti and TiC, TiN and TiCN (Arockiasamy et al., 2011) and the essentially ionic character of TiX (where X could be B, C, N, O, Si, P or S) bonds with only minor covalency between non-metal ions [23] are essential to explain high density even at relatively low sintering temperature.

Figure 3a and b show fine and coarse morphologies for TiC at the grain boundaries whereas in the case of TiN (fig. 3c) an extended diffusion of nitrogen in titanium is observed at lower amount of TiN. However, this does not seem to be the case when the amount of TiN is increased up to 5 wt. %. These results are in agreement with those obtained by Wood (Wood, 1974) who stated that titanium nitride constitutes a diffusion barrier to nitrogen diffusion. This correlates very well with the slight decrease in density as the amount of TiN is increased. Furthermore, both the α-Ti and β-Ti phases easily dissolve nitrogen than carbon [19] which may result in the formation N_2 gas which results in pore formation. This seems to justify the high level of pores in Figure 3f as a result of the increased amount of TiCN.

The presence of of a high level of pores especially in Figure 3g and h explains the lower density of Ti/TiB_2 as a result of lower bonding which results in easy pull out during sample preparation.

To gain insight into the structure, the optical microscope (OM) micrographs of Ti without and with additives sintered at 950^0C were recorded as shown in Figure 4.

This figure shows a microstructure with evenly distributed titanium-based ceramics. Figure 4a which shows the microstructure of cP-Ti, reveals few small equiaxed grains along with elongated and large grains. Figures 4b-d-f and c-e-g show the microstructures of the samples with 2.5 and 5% Ti-based ceramic additives respectively. The two cases result in a finer microstructure as compared to cP-Ti and the reduction of the grains is more evident in the case of 5% addition. This illustrates the inhibitive behaviour of the ceramic additives to grain growth [24]. Smaller grains can also be observed as the amount of the additives is increased. This is probably due to the facilitation of surface diffusion during sintering as a result of the interactions between Ti and TiC, TiCN and TiN. This has resulted in a homogenized microstructure as pointed out by Arockiasamy et al. [25].

The inter diffusion between Ti and the ceramic additives may lead to a solid solution transition zone which results in an improved densification. However, in the present work the observed decrease in density with the additives may suggest that the sintering temperature considered is not high enough to promote high degree of inter diffusion as compared to the work by Fujii et al. [26].

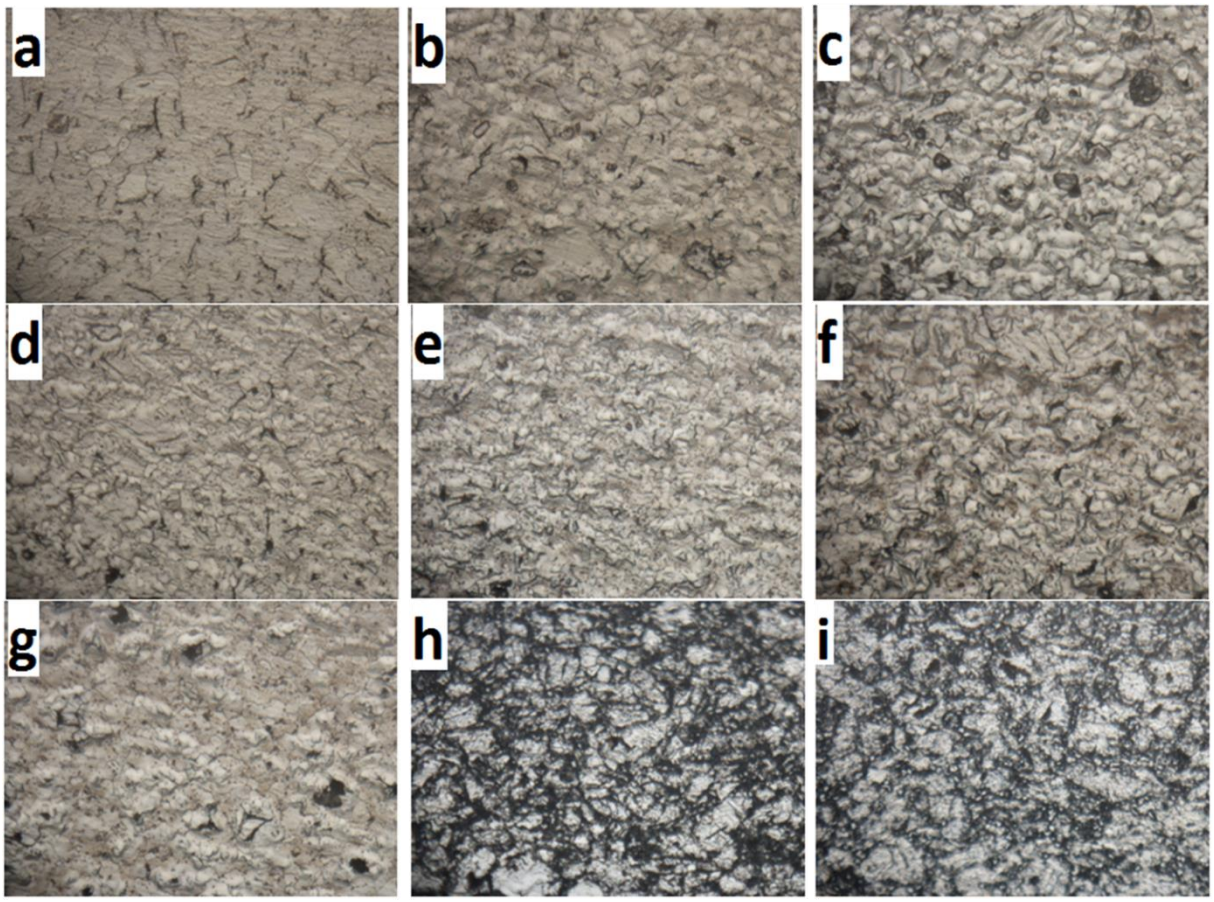

Figure 4. Optical micrographs of a) Ti; b) Ti-2.5TiC; c) Ti-5TiC; d) Ti-2.5TiN; e) Ti-5TiN; f) Ti-2.5TiCN, g) Ti-5TiCN, h) Ti-2.5TiB_2 and i) Ti-5TiB_2 (Magnification x 50)

Though the addition of TiB_2 resulted also in a finer microstructure as compared to that of CP-Ti, the grain size associated with its addition are bigger than those obtain with the addition of TiC, TiN and TiCN. An increase in the amount of TiB2 (from 2.5 to 5 wt. %) leads to bigger grains. TiB_2 inhibits grain growth only to a lesser extent as compared to TiC, TiN and TiCN. The increase in the amount of TiB_2 seems to decrease the inhibitive nature of the additive to grain growth. This may be explained by the anisotropic nature of TiB2 (hexagonal grain structure) which may result in detrimental internal stresses and the onset of spontaneous micro cracking during cooling [27].

XRD measurements

The XRD spectra of the samples with and without additives are shown in Figures 5 (2.5 wt. % additives) and 6 (5 wt. % additives).

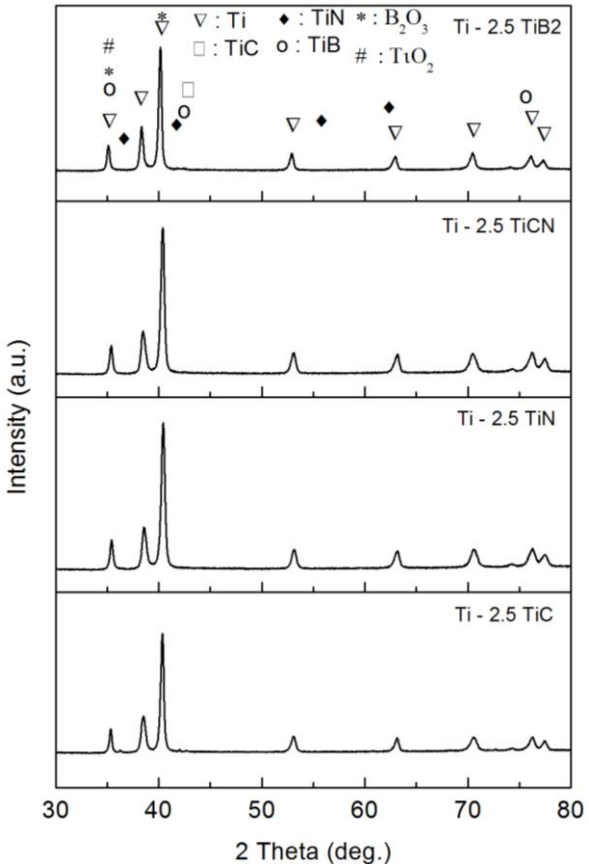

Figure 5. XRD plots of spark plasma sintered Ti with 2.5 wt. % of TiC, TiN, TiCN and TiB_2

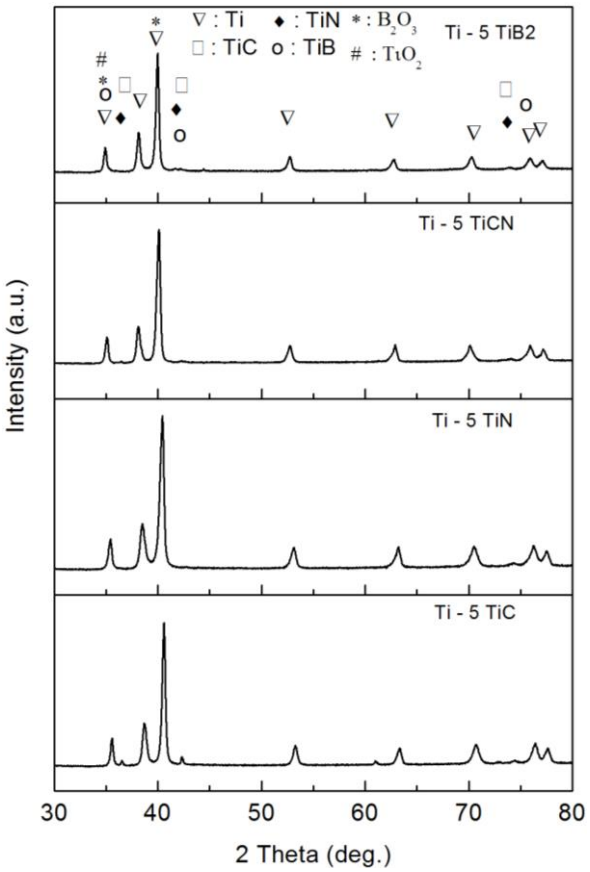

Figure 6. XRD plots of spark plasma sintered Ti with 5 wt. % of TiC, TiN, TiCN and TiB_2

In the samples obtained by adding TiC and TiN to Ti, no structural change was found but C and N diffusion is expected to occur during sintering which may result in the reduction on the amount of TiC and TiN. Carbon and nitrogen, besides their solid strengthening effect as alfa phase stabilizers, have different individual effects on the mechanical properties [28]. In the case of TiB_2 and TiCN, phase decomposition did occur leading to TB and TiC and TiN, respectively and the presence of TiO_2 and B_2O_3 phases was observed. The in-situ formation of TiB within the matrix may be obtained from the reaction $Ti+TiB_2 = 2TiB$.

This reaction, according to Zhang et al. [29], is favored to form as long as there is excess Ti (or if the total boron average content is below 18 wt. %) despite its slightly negative Gibb's free energy of formation, compared to other reactions.

Effect of the additives on hardness

The effect of TiC, TiN, TiCN and TiB_2 additions and their amounts on micro hardness (HV) is shown in Figure 7.

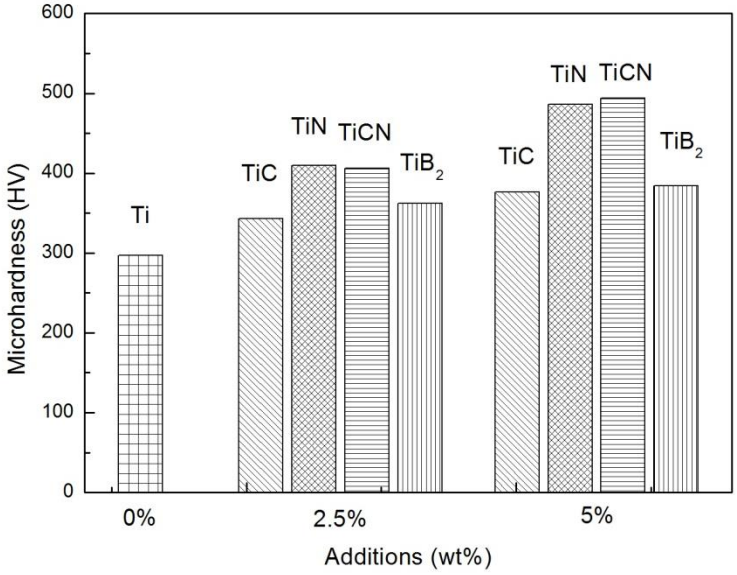

Figure 5. Effect of TiC, TiN, TiCN and TiB_2 additions on hardness of cP-Ti

TiC, TiN, TiCN and TiB_2 additions cause an increase of micro hardness which is further improved when the amount of the additives is higher. In all the cases TiC addition has the lowest micro hardness while TiN and TiCN improve much better with close values. The micro hardness values associated with the addition of TiB_2 lies between those of TiC, TiN and TiCN. The increase in micro hardness can be explained by the high hardness nature of the additives. It is worth noting also that, as observed from the micrographs in Figure 4, the additives are segregated at grain boundaries, thereby inhibiting grain growth and therefore further improving micro hardness. Despite the higher hardness of TiC compared to that of TiCN and TiN, its addition in Ti gives a lower hardness. This could be due to the presence of nitrogen in the case of TiN and TiCN which is more easily dissolved by Ti compared to carbon. Previous work [30] has also demonstrated that spallation of pure TiC may occur due to high internal compressive stress whereas TiCN offers good coating-substrate adhesion.

Fracture surface analysis

The fracture images of both Ti samples with and without additives sintered at 950^0C are shown in Figure 8.

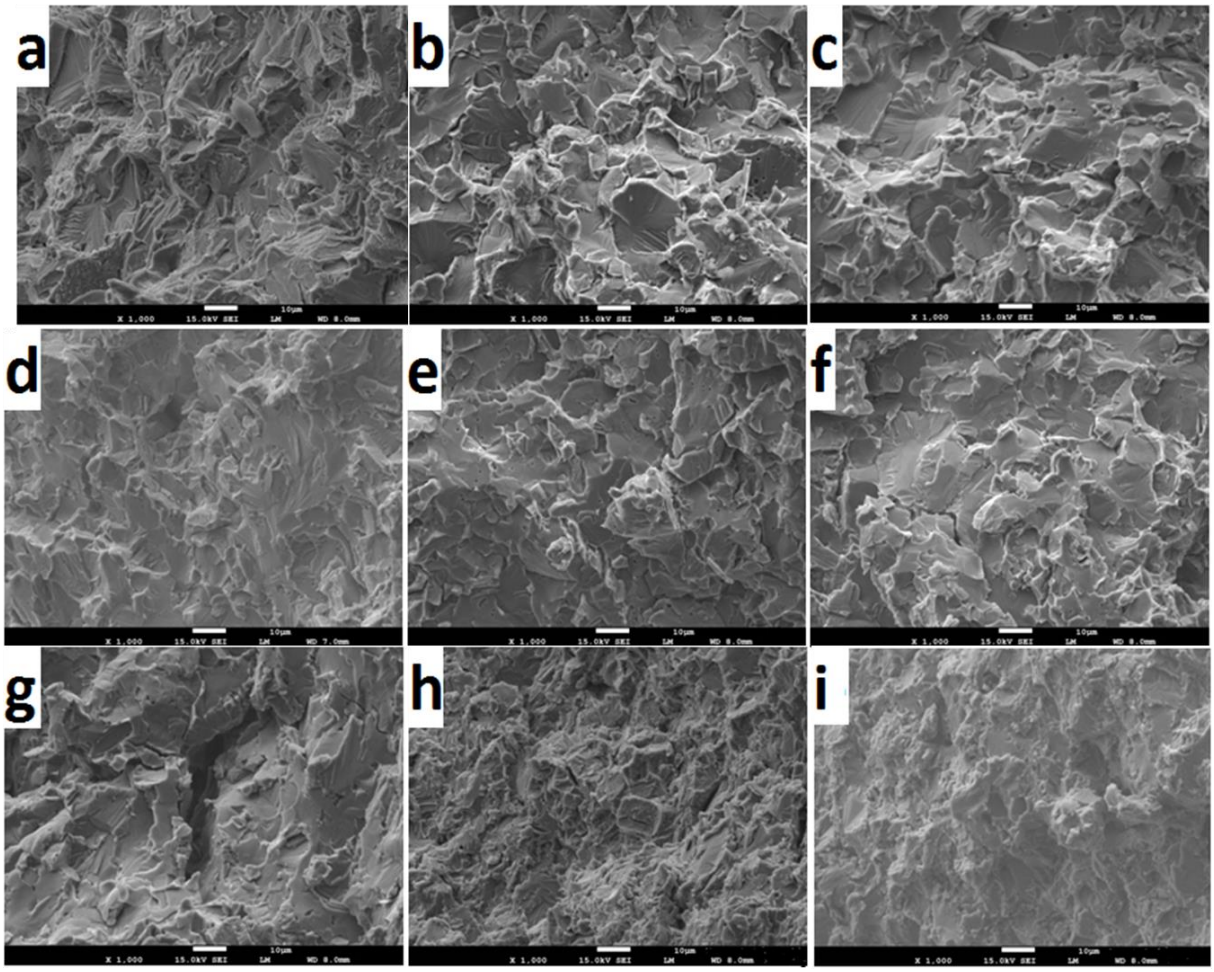

Figure 6. Fracture micrographs of a) Ti; b) Ti-2.5TiC; c) Ti-5TiC; d) Ti-2.5TiN; e) Ti-5TiN; f) Ti-2.5TiCN, g) Ti-5TiCN, h) Ti-2.5TiB_2 and e) Ti-5TiB_2

In Ti without additive both inter- and intra-granular fracture modes are present with a predominance of the latter. In the Ti with additives the opposite is noticed which suggests weak grain boundary structures. The fracture mechanism in all the different situations is mainly of trans granular cleavage and crack propagation occurring through the grains. The presence of residual porosity within the grain boundary, as observed in the samples with additives, and the local stress [31] weaken the grain boundaries and making them a route for crack propagation. The cracks observed in Figure 4c, f, g and h correlate very well this.

Conclusions

In the present work, the processing of titanium matrix composites from pure titanium and titanium-based ceramics additives using spark plasma sintering was considered.

The study of the effect of the additives on density, densification behaviour, microstructure and hardness of Ti has been carried out. The following conclusions can therefore be derived:

- The addition of TiC, TiN, TiCN to Ti resulted in overlapping between localized and bulk deformation whereas that of TiB_2 follows the same trend of pure Ti.
- Relative densities ranging from 97.8 to 99.6% were achieved at a relatively low sintering temperature of 950^0C.
- The inhibitive behavior of the additives to grain growth is clearly identified and is believed to be the cause for the improved hardness besides the hard nature of the additives.
- The high improvement on hardness of TiCN is believed to result from the combine effect of TiC and TiN.
- The addition of the titanium-based ceramics change the fracture mode from trans granular to intergranular

Acknowledgments

This research is supported by the Institute for Nano Engineering Research, Department of Chemical and Metallurgical Engineering, Tshwane University of Technology.

References

1. Lieberman S.L., Gokhale A.M., Tamirisakandala S., Bhat R.B., Three-dimensional microstructural characterization of discontinuously reinforced Ti64–TiB composites produced via blended elemental powder metallurgy, Mater. Charact., 2009, 60, p. 957–963.
2. Zadra M., Girardini L., High-performance, low-cost titanium metal matrix composites, Mater. Sci. Eng. A, 2014, 608, p. 155–163.
3. Boyer R, Welsh G.E.W, Collings, Materials Properties Handbook: Titanium Alloys, ASM International, 1994.
4. Akkaya S.S, Vasyliev V.V., Reshetnyak E.N., Kazmanlı K., Solak N., Strel'nitskij V.E., Ürgen M., Structure and properties of TiN coatings produced with PIII&D technique

using high efficiency rectilinear filter cathodic arc plasma, Surf. Coat. Technol., 2013, 236, p. 332-340.

5. Yun E., Lee K., Lee S., Correlation of microstructure with high-temperature hardness of (TiC, TiN)/Ti-6Al-4V surface composites fabricated by high energy electron-beam irradiation, Surf. Coat. Technol., 2005, 191, p. 83-89.
6. Wu Y., Wang A.H., Zhang Z., Xia H.B., Wang Y.N., Wear resistance of in situ synthesized titanium compound coatings produced by laser alloying technique, Surf. Coat. Technol., 2014 258, p. 711-715.
7. Makuch N., Kulka M., Dziarski P., Przestacki D., Laser surface alloying of commercially pure titanium with boron and carbon, Opt. Lasers. Eng., 2014, 57, p. 64-81.
8. Yazdi R., Kashani-Bozorg S.F., Microstructure and wear of in-situ Ti/(TiN + TiB) hybrid composite layers produced using liquid phase process, Mater. Chem. Phys., 2015, 152, p. 147-157.
9. Yang Y., Yao W., Zhang H., Phase constituents and mechanical properties of laser in-situ synthesized TiCN/TiN composite coating on Ti-6Al-4V, Surf. Coat. Technol., 2010, 205, p. 620–624.
10. Gülsoy H.O., Gunay V., Baykara T., Influence of TiC, TiN and TiC(N) additions on sintering and mechanical properties of injection moulded titanium based metal matrix composites, Powder Metall., 2015, 58(1), p. 30-35.
11. Coetzel C.G., Treatise on powder metallurgy, Interscience publishers, New York, 1949.
12. Sommier N., Porion P., Evesque P., Leclerc B., Tchoreloff P., Couarraze G., Magnetic resonance imaging investigation of the mixing–segregation process in a pharmaceutical blender, Int. J. Pharm., 2001, 222, p. 243–258.
13. Zadra M., Casari F., Girardini L., Molinari A., Spark plasma sintering of pure aluminium powder: mechanical properties and fracture analysis, Powder Metall, 2007, 50(1), p. 40–45.
14. Zadra M., Casari F., Girardini L., Molinari A., Microstructure and mechanical properties of cp-titanium produced by spark plasma sintering, Powder Metall., 2008, 51(1), p. 59–65.
15. Liu D., Xiong Y., Li Y., Topping T.D., Zhou Y., Haines C., Paras J., Martin D., Kapoor D., Schoenung J.M., Lavernia E.J., Spark Plasma Sintering of Cryomilled Nanocrystalline Al Alloy - Part II: Influence of Processing Conditions on Densification

and Properties, Metall. Mater. Trans A: Phys. Metall. Mater. Sci., 2012, 43, p. 340–350.

16. Xiong Y., Liu D., Li Y., Zheng B., Heines C., Paras J., Martin D., Kapoor D., Lavernia E.J., Schoenung J.M., Spark Plasma Sintering of Cryomilled Nanocrystalline Al Alloy - Part I: Microstructure Evolution. Metall. Mater. Trans. A: Phys. Metall. Mater. Sci., 2012, 43, p. 327–339.
17. Groza J.R., Zavaliangos A., Sintering activation by external electrical field, Mater. Sci. Eng. A, 2000, 287, p. 171–177.
18. Anselmi-Tamburini U., Gennari S., Garay J.E., Munir Z.A., Fundamental investigations on the spark plasma sintering/synthesis process: ii. Modeling of current and temperature distributions, Mater. Sci. Eng. A, 2005, 394(1-2), p. 139–148.
19. Vanmeensel K., Laptev A., Hennicke J., Vleugels J., Van der Biest O., Modelling of the temperature distribution during field activated sintering, Acta. Mater, 2005, 53, p. 43-79
20. Diouf S., Molinari S., Densification mechanisms in spark plasma sintering: Effect of particle size and pressure Powder Technol., 2012, 221, p. 220–227.
21. Diouf S, Fedrizzi A, Molinari A, A fractographic and microstructural analysis of the neck regions of coarse copper particles consolidated by Spark Plasma Sintering, Mater. Lett, 2013, 111, p. 17–19.
22. Agarwal A., Katipelli L.R., Dahotre N.B., Elevated temperature oxidation of laser surface engineered composite boride coating on steel, Metall. Mater. Trans. A, 2000, 31, p. 461–473.
23. Chen K, Kamran S, Bonding Characteristics of TiC and TiN, Model. Num. Sim. Mater. Sci., 2013, 3, p. 7-11.
24. Knotek O., Löffler F., Krämer G., Arc deposition of TiC and TiCN using acetylene as a reactive gas, Vacuum, 1992, 43(5-7), p. 645-648.
25. Arockiasamy A., German R.M., Heaney D.F., Wang P.T., Horstemeyer M.F., King R.L., Adcock B., Effect of additives on sintering response of titanium by powder injection moulding, Powder Metall, 2011, 54, p. 420–426.
26. Fujii H., Fujisawa K., Takahashi K., Yamazaki T., Development of low cost powder metallurgy process of titanium alloy products', Nippon Steel Technical. Rep., 2002, 85.
27. Munro R.G., Material properties of titanium diboride, J. Res. Nat. Inst. Stand. Technol., 2000, 105, p. 709-720.
28. Finlay W.L., Snyder J.A., Effects of Three Interstitial Solutes (Nitrogen, Oxygen and

Carbon) on the Mechanical Properties of High-purity Alpha Titanium, J. Metals, 1950, 188, p. 277-286.

29. Zhang X., Lu W., Zhang D., Wu R., In situ technique for synthesizing (TiB+TiC)/Ti composites, Scripta Mater., 1999, 41(1), p. 39.
30. Fu Y., Du H., Sun C.Q., Interfacial structure, residual stress and adhesion of diamond coatings deposited on titanium, Thin Solid Films, 2003, 424, p. 107–114.
31. Huai K.W., Guo J.T., Gao Q., Li H.T., Yang R., Microstructure and mechanical behavior of NiAl-based alloy prepared by powder metallurgical route, Intermetallics, 2007, 15, p. 749–752.